Journal of New Results in Science (JNRS)

ISSN: 1304-7981
http://dergipark.gov.tr/en/pub/jnrs
Research Article
Open Access

Volume: 9
Issue: 1
Year: 2020
Pages: 53-62

Received: 18.04.2020 ***Accepted***: 06.05.2020

Investigation of the Effect of Aggregate Obtained from Çatakören Region in Bolu on the Crucial Properties of Conventional Concretes

Bahattin Öztoprak*

Yenicağa Yaşar Çelik Vocational High School, Bolu Abant Izzet Baysal University, Bolu, Turkey
**Corresponding author, bahattin.oztoprak@ibu.edu.tr*

ABSTRACT: This current study delved into the not only meticulous characterization of the aggregate obtained from Çatakören region in Bolu but also its usage potential in the production of traditional concretes. The compressive strength, slump grade, apparent density of the three types of prepared concretes (C25/30, C30/37 and C35/45) as well as microstructural properties of the fractured samples via SEM were investigated in detail. Furthermore, all the characteristic properties of the component such as cement, set accelerating admixture, water reducing admixture and the aggregates were determined with the aid of analyses carried out according to the relevant standards. As for the aggregate, the physical, qualitative mineralogical, petro-graphic, X-ray diffraction, mechanical besides the grain size distribution limits properties of the aggregates investigated successfully. In the light of these analyses, it was found that the aggregates produced from Çatakören region was considerable proper and had more usability potential for the production of the traditional concretes meeting the standards. Additionally, among the produced concrete samples, the maximum compressive strength value, 51.3 MPa were obtained from C35/45 concrete samples as expected due to the usage of the relatively larger amount of cement and admixture in the production of this concrete. SEM analyses also showed that the formation of better interfacial adhesion and stronger chemical bonds, especially in C-S-H were formed in the concrete matrix due to the probable decrement in the porosity. Furthermore, it was apparent from the images that there existed voids, space, ettringites, microcracks besides the structures regarding as C-H and C-S-H in the concrete matrix.

Keywords – *Çatakören aggregate properties, Compressive strength, Slump grade, Apparent density, Morphological properties*

1. Introduction

It is well-known the fact that concrete is commonly used building material encountered almost everywhere in our daily life. Concrete can be defined as the mixture material composed of cement (7-15%), water (14-18%), fine aggregate (24-28%), coarse aggregate (30-50%) and, if necessary, mixing of additives together (not exceeding 5% of the cement dosage to the concrete), which have easily shapeable characteristics. While cement and water form cement paste, fine and coarse aggregate form the aggregate composition. In addition, there exists a certain amount of air (0.5-8%) in the concrete. Concrete has the unique features such as durability, safety, economy, easily shapeable, low maintenance, low energy production and aesthetics (Stroeven and Hu, 2006). Due to these features, it is highly preferred in construction of concrete housing, bridge, road, barrier, dam, tunnel, etc. As such, one of the main goals of scientists was to improve the physical properties of concrete building material (Gencel, 2011; Kakae et al., 2017). For this purpose, many different types of materials have been developed by reinforcing the concrete with the usage of the varying types of aggregates (Eui-Hwan et al., 2007; Evangelista et al., 2015). Aggregates are used in concrete production with the help of binders and make up approximately 70-75% of the concrete. Aggregates can be obtained as a result of breaking large pieces of stone in stone crushers as well as they are naturally found in nature. The aggregates obtained in the crusher are called as fine or coarse aggregates. Fine aggregates having larger size compared to coarse aggregates can be used separately or together with coarse concretes in the concrete. In other words, the aggregates used in the concretes plays an significant role in the physical, mechanical due to the formation of the bonds between coarse aggregates and cement paste, leaching, chemical and morphological properties of the formed concrete (Liu et al., 2019; Lyu et al., 2019; Ramdani et al., 2019). The geometric shapes of aggregate grains also affect the workability of concrete (Leman et al., 2017; Sokhansefat et al., 2019). Furthermore, the geometric shapes of aggregate grains also affect the workability and mechanical properties of concrete (Roy et al., 2020; Ueno and Ogawa, 2020). The need for water increases in concretes made with angled aggregates, but relatively good adherence is obtained between aggregate grains and cement paste. Due to the lack of sufficient cement paste during the mixture, the surface of the aggregate is not fully wrapped with cement paste and the friction of the aggregates occurs. Since the ratio of aggregate surface to volume in angled aggregate grains is quite large, a lot of cement paste is needed to cover the surface of aggregate grains. Due to the excessive changes in the aggregate geometry, the internal stress occurs in the concrete, which affects negatively the mechanical properties of the concrete. As for mechanical properties, the materials such as concrete, polymer, composites etc. having relatively high compatibility between components showed larger mechanical performance (Liu et al., 2016; Sahin and Akarsu, 2011; Soykan and Cetin, 2015). Thus, in order to obtain better mechanical properties in the concretes, the spatial geometry of the aggregate becomes more suitable to form relatively more stronger interactions between cement paste and aggregates. Accordingly, Halvaei et. al. studied the effect of acrylic fibers with different shapes and tensile strengths selected as reinforcement of the specific fine aggregates concrete on the concrete mechanical properties. They found that the flexural toughness and pullout strength were increased 20% and 34% with the usage of the acrylic fibers having the optimum shapes, respectively (Halvaei et al., 2016). In addition to the shape of aggregate, the mineralogical structure of the aggregate affects the strength of the bond between the aggregate and the cement paste since there exists a chemical bond between aggregate and cement paste. Herein, it is to be stated that mineralogical content of the aggregates is highly depended on the region at which the aggregates are extracted. Accordingly, the region and source of the aggregates changes the varying properties of the concretes as reported in previous studies (Aksut and Yetgin, 2017; Campelo et al., 2019; de Oliveiraet al., 2019; Marthong et al., 2017).

As seen in the literature investigation, the type, source, region and shape of the aggregates had large influence on the concrete characteristics. In the light of that, in this current study, not only the characterization of the aggregates obtained from the Çatakören region in Bolu were performed but also the effects of this aggregates on the different type of concretes (C25/30, C30/37 and C35/45) were investigated for the first time.

2. Material and Methods

2.1. Material

The aggregate obtained from crushed stone located Çatakören region in Bolu city were supplied from Bolu Cement Factory for this present study. CEM I 42.5 R cement used in concrete mixtures as a binder, the set accelerating admixture and the water reducing admixture were supplied from Bolu Ready-Mixed Concrete Facility. The physical and chemical properties of this used cement and the admixtures used in the concrete are given according to the relevant standard in Table 1, 2 and 3, respectively.

Table 1. Chemical and physical properties of the cement

CHEMICAL PROPERTIES						
Order No	Test Name	Values obtained (%)			Limit Values TS EN 197-1	Experiment Methods
		Time 1	Time 2	Time 3		
01	Sulfur Trioxide (SO_3)	2,79	2,81	2,78	Max. 4,0	TS EN 196-2
02	Chloride (Cl-)	0,0262	0,0254	0,0267	Max. 0,10	TS EN 196-2
03	Loss of ignition	2,91	2,97	2,88	Max.5,0	TS EN 196-2
04	Insoluble Residue	0,73	0,77	0,79	Max.5,0	TS EN 196-2
05	Sodium Oxide (Na_2O)	0,26	0,25	0,29	---	TS EN 196-2
06	Potassium Oxide (K_2O)	0,64	0,59	0,66	---	TS EN 196-2
07	Total Alkali (Na_2O Equivalent)	0,69	0,63	0,71	---	TS EN 196-2
PHYSICAL PROPERTIES						
01	Specific gravity (gr/cm^3)	3,15	3,15	3,15	---	TS EN 196-6
02	Specific Surface (cm^2/g)	4096	4087	4099	---	TS EN 196-6
03	Initial set (Munite)	112	114	110	Min. 60	TS EN 196-3
04	Volume Expansion (Le chatelier) (mm)	1	0.9	0,9	Max.10	TS EN 196-3
05	2 Day Compressive Strength (MPa)	28,7	27.9	29,3	Min. 20	TS EN 196-1
06	28 Day Compressive Strength (MPa)	56,1	58.0	57,4	Min. 42,5-Max. 62,5	TS EN 196-1

Table 2. Characteristic properties of the set accelerating admixture

Experiment Name	Results			Standard Values	Analysis Method
	Time 1	Time 2	Time 3		
Homogeneity	Homogenous	Homogenous	Homogenous	Homogenous	With eye
Color	Brown	Brown	Brown	Brown	With eye
Relative Density (g/cm3)	1,18	1,16	1,17	1,15-1.21	ISO 758
pH	5,4	5,1	5,7	4,0-6,0	ISO 4316
Solid Content (%)	25,33	25,12	25,56	24,25-26,80	EN 480-8
Water Soluble Chloride (%)	0,06	0,04	0,07	<0,1	EN 480-10
Alkali Amount (%)	Suitable	Suitable	Suitable	<5	EN 480-12
FTIR Spectrum / Active Component	Suitable	Suitable	Suitable	Referans IR Spect.	EN 480-6

Table 3. Characteristic properties of the water reducing admixture

Experiment Name	Results			Standard Values	Analysis Method
	Time 1	Time 1	Time 1		
Homogeneity	Homogenous	Homogenous	Homogenous	Homogenous	With eye
Color	Brown	Brown	Brown	Brown	With eye
Relative Density (g/cm3)	1,12	1,10	1,11	1,09-1.15	ISO 758
pH	5,7	5,3	5,8	4,0-6,0	ISO 4316
Solid Content (%)	26,18	26,38	26,62	25,77-28,48	EN 480-8
Water Soluble Chloride (%)	0,06	0,03	0,06	<0,1	EN 480-10
Alkali Amount (%)	Suitable	Suitable	Suitable	<5	EN 480-12
FTIR Spectrum / Active Component	Suitable	Suitable	Suitable	Referans IR Spect.	EN 480-6

2.2. Methods

In this current study, first of all, the characterization of the both fine and coarse aggregates taken from the predetermined certain area of the Çatakören region located at Bolu were performed with the usage of the conventional experimental methods carried out in Experimental Laboratory in Turkish Ready Mixed Concrete Association and Mineral Analysis and Technology Department in Mineral Research and Exploration General Directorate (MTA) with the usages of the relevant standards. The production of concretes was carried out completely automatically by managing via remote control with the usage of computer. The aggregates were weighed twice in the automatic scale, one rough and sensitive, and poured on the conveyor belt, then went to the mixer chamber. The weighed water and chemical additive mixed together, then went to the mixer while Cement was weighed individually and added directly to the mixer. Efficiently mixed concrete was transformed into the trans-mixer in order to carry easily the concrete. The samples were taken time to time so as to determine the properties of the concrete such as the temperature and slump value. The prepared concrete samples were placed in the three-chamber prism mold (150x150x150mm). Concrete samples in the mold were waited for 26 day by keeping the sample in the curing pool, as being totally 28 days for the compressive tests. After the removal the concrete samples from the curing pool and, the samples left in room conditions for 1 day. The real amounts of the components composed of the concretes were tabulated in Table 4. The analysis of the compressive strengths, slumps and apparent densities properties of prepared C25/30, C30/37 and C35/45 concrete samples was conducted according to the relevant standards. The obtained values were given as the average value of the 15 experimental tests for each concrete sample.

Table 4. The actual concrete mixture values

Concrete Actual Mixture Values (kg/m^3)			
	C25/30	C30/37	C35/45
Cement	300	335	390
Water	165	184	160
Crushed Sand	995	962	967
Crushed Stone I	344	333	335
Crushed Stone II	555	536	540
Admixture	3	3,685	5,46
Total	2.366	2.356,685	2.402,46

2.3. Instruments

Further, the fractured surface morphology of the concrete samples was investigated by using scanning electron microscope (SEM) FEI–Quanta FEG 250, operated at 10 kV in the secondary electron image (SEI) mode with a resolution power of 3 nm.

3. Results and Discussion

3.1. The Characterization of the Aggregate

Prior to discussion on the results, it was to be stated the map location of the region where the aggregate was obtained. As seen in Fig. 1, this region is located in the north-west of Çatakören on Mengen road.

Fig. 1. Map location of the region where the aggregate was obtained

In order to figure out the physical, qualitative mineralogical and petro-graphic and mechanical properties of the used aggregate obtained from Çatakören region, both the coarse and fine aggregate (crushed sand, crushed stone I, crushed stone II) samples were characterized in detail. The obtained characteristic properties of the aggregate were given in Table 5-8.

Table 5. The physical analysis results of the aggregates

Experiment Name		Results (%)			Limit Values	Standard
		Time 1	Time 2	Time 3		
Flatness Index (Aggregate I)		9,0	8,7	9,2	FI15 (≤15)	TS EN 933-3:2012
Flatness Index (Aggregate II)		7,0	7,3	7,7	FI15 (≤15)	TS EN 933-3:2012
Abrasion of Coarse Aggregates (Los Angeles) Aggregate I and II (Applied to aggregate in the range of 10-14mm)		16,0	15,5	16,6	LA20 Max. %30	TS EN 1097-2:2010
Drying creep		0,035	0,037	0,036	---	TS EN 1367-4:2009
Alkali Silica Reactivity	3 Day	<0,01	<0,01	<0,01	---	ASTM C 1260-14
	7 Day	0,01	0,01	0,01	---	ASTM C 1260-14
	14 Day	0,01	0,01	0,01	Harmless	ASTM C 1260-14

Table 6. Qualitative mineralogical and petro-graphic analysis results of the aggregate

Macroscopic Identification	Results		
	Time 1	Time 2	Time 3
Colour	Yellowish Gray (5Y8/1 Geologial Rock- Color Chart 2009)	Yellowish Gray (5Y8/1 Geologial Rock- Color Chart 2009)	Yellowish Gray (5Y8/1 Geologial Rock- Color Chart 2009)
Texture	clastic	clastic	clastic
Particle size	Small - Medium - Coarse	Small - Medium - Coarse	Small - Medium - Coarse
Main components	Fossil limestone fragments, Epiclastic material, Carbonate minerals (Carbonate cement)		
Fossil Limestone Parts	It consists of medium grained, microfossils and shells (micro-cryptocrystalline or micro-mesocrystalline carbonate mineral filled) and crypto-microcrystalline carbonate binder. Some of them contain small amounts of microfossils and shells.		
Epiclastic Material	Small grain, quartz, chlorite and opaque mineral grain as lesser extent		
Baking Soda Cement	Small grain (micritic, sometimes sparitic) carbonate minerals		
Filled Fractures and Veins	0.8 -0.08 mm grain size width, parallel and intersecting each other		
Fillers	Small grain (micro-meso crystalline) filled with carbonate minerals		

Table 7. XRD analysis results of the aggregates

X-Ray Diffraction (XRD)	Results		
	Time 1	Time 2	Time 3
Rock name	Calcirudite	Calcirudite	Calcirudite
Calcite	Dominant	Dominant	Dominant
Dolamite	Little	Little	Little
Quartz	Little	Little	Little
Chlorite Group Mineral	Little	Little	Little
Kaolinite Group Clay	Little	Little	Little

Table 8. Mechanical properties results belonging to crushed sand, crushed stone I, crushed stone II existing in the aggregates

Experiment Name	Results (g/cm^3)		
	crushed sand	crushed stone I	crushed stone II
Apparent Grain Density	2,70	2,72	2,67
Drying Grain Density	2,54	2,65	2,65
Dky Grain Density	2,61	2,67	2,66
Water Absorption	2,30	0,90	0,34
Porosity%	5,8	2,4	1
Composition%	94,2	97,6	99

Additionally, the results regarding the percentage of fine material analysis belonging to the crushed sand, crushed stone I, crushed stone II were recorded as average value of 5.6%, 0.8% and 0.7%, respectively. Furthermore, the analysis showed that the aggregate size, bulk density and tapped density values belonging to the crushed sand, crushed stone I, crushed stone II components existed in the aggregate were found to be 0-4 mm, 4-11.2 mm, 11.2-22.4 mm; 1.851 kg/dm3, 1.630 kg/dm3, 1.563 kg/dm3 and 2.105 kg/dm3 , 1.768 kg/dm3 , 1.651 kg/dm3, respectively. Moreover, so as to determine the level of the impurity presenting in the crushed sand, the percentage of the methylene blue analysis were conducted with 3 times at the varying intervals. The obtained findings depicted that the percents methylene blue of the crushed sand were found to be 0.5%, 0.7% and 0.8% and these values were relatively smaller than the limit value (1%).

The determination of the grain size distribution of aggregate by gradation analysis were also carried out according to the method in TS 3530 EN 933-1 (1999). The results regarding to the size distribution of the aggregate putting into the mixture were tabulated numerically in Table 9 and the obtained gradation curve corresponding to aggregate's granulometrical character was also drawn in Fig. 2. The aggregates samples presenting between the standard curves depicted that the amount of fine and coarse aggregates was close to each other.

Table 9. The grain size distribution limits of the aggregate

sieves		(%) passing through sieve		
inç	mm	I	II	III
1¼"	31,5	100,0	100,0	100,0
7/8"	22,4	100,0	100,0	100,0
5/8"	16,0	100,0	100,0	49,0
1/2"	12,5	100,0	100,0	22,0
5/16"	8,0	100,0	52,0	2,0
#5	4,0	93,0	-	2,0
#10	2,0	56,0	3,0	2,0
#18	1,0	34,0	3,0	2,0
#35	0,5	25,0	3,0	2,0
#60	0,25	20,0	3,0	2,0
#120	0,125	14,0	3,0	2,0
#230	0,063	10,0	0,9	0,5
fineness		**3,6**	**6,3**	**7,4**

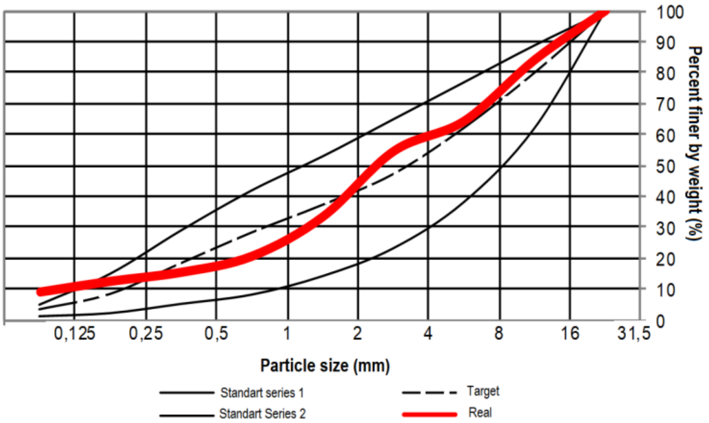

Fig. 2. Gradation curve of aggregate obtained from Çatakören region

3.2. The Analysis of the Compressive Strength of the Concretes

Prior to discussions, the compressive strengths of the produced concrete samples (C25/30, C30/37 and C35/45) were determined to figure out the resistance of the concretes to breaking under compression. The variation of the compressive strengths of the concrete samples regarding the role of the aggregates were depicted in Fig. 3. It can deduced from the figure that all concrete samples had the values that were comparatively larger than the value indicated in the relevant standards. Furthermore, the compressive strengths for C25/30, C30/37 and C35/45 concretes were found to be 37.5, 42.5 and 51.3 MPa, respectively. These results depicted that the used aggregate obtained from the Çatakören region was apparently suitable for the production of the concrete having desired properties. Moreover, these consistent increments (as expected) were believed to caused by the enhancements in the distribution of C-S-H gel in the hardened cement paste. Additionally, the another reason concerning the almost linearly increase was probably caused by the relatively lower decrement in the porosity due to the increment in the amount of cements and admixtures in the C35/45 concrete sample, which results in the maximum value in the compressive strength.

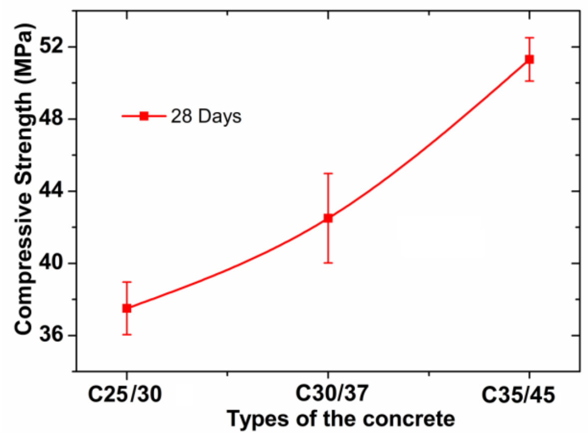

Fig. 3. The variation of the compressive strengths of the produced concrete samples

3.3. Slump and Apparent Density Analysis of the Concretes

In this part of this current study, slump and apparent density analyses of the concretes were performed in order to determine both the workability and consistency of the prepared concrete mixtures. The obtained results were given numerically in Table 10. It is known that the concrete slump values indicates the cement/water ratio as well as gives a sign regarding the other components (admixtures, aggregate etc.) presenting in the concretes. The obtained result exhibited that all the concrete samples possessed S3 slump grades according to TS EN 206-1, which means that the slump range of the samples were in the range from 100 to 150 mm. As for the apparent density, all the concrete samples had the same values and this value was recorded approximately as 2.380 kg/m3.

Table 10. The slump grade and apparent density results belonging to the concrete samples

	C25/30	**C30/37**	**C35/45**
Slump grade	S3	S3	S3
Apparent density (kg/m^3)	2.380±0.007	2.379±0.007	2.379±0.013

3.4. Morphological Properties of the Concretes

The morphological properties of the fractured surfaces obtained from the compressive strengths tests of C25/30 and C30/37 concrete samples were investigated meticulously by means of SEM analysis. The taken SEM images obtained at 2000 and 3000 magnification scales were illustrated in Fig. 4.The obtained images given as a, b, and d showed the changes in C25/30, while the fractrographs indicated as e, f, g and h were belonging to C30/37 concretes. The surface fractographs showed that, at the C30/37 concrete sample, more effective C-S-H gel was greatly spread throughout the mixtures of hydrated cement paste, which brings about the high strength. This was presumably caused by that the amount of the used cement and admixture were comparatively large compared to C25/30. Furthermore, since the amount of aggregates used in the production in C25/30 concretes (See. Table 4) was higher than C30/37 concretes, it was observed form the images that C-S-H formation in C25/30 concretes was completed better with sufficient chemical reactions, which results in the comparatively inadequate strength in the concrete. Moreover, it was obvious that the porosity of C30/37 concrete was comparatively lower comparing to C25/30 concrete. This observation also revealed why C30/37 concrete had larger compressive strength than C25/30 concrete. Additionally, when examining the fractograph b and f, it was obvious that the formation of voids, pores and spaces in C25/30 concrete encountered more frequently compared to C30/37 concrete. Furthermore, the roughly spherical voids were observed in SEM images of C25/30 concrete due to the water evaporation in the concrete matrix, Fig. 4.c. This space formation was gradually lower in C30/37 concrete, in Fig. 4.g. The needle-like particles, in other words ettringites, were also explicitly detected from the SEM images in Fig. 4. c, d, g and h. The another results deduced from the SEM analysis was that the micro structures caused by C-H and C-S-H (both honey-comb and fibrous) were formed in the both classes of the concretes matrices, especially in Fig. c and g. Moreover, the microcracks propagated along the concrete matrices were seen in the taken SEM images, which forms during the compressive tests. All in all, C20/25 concrete apparently possessed the better morphological properties than that C30/37 had.

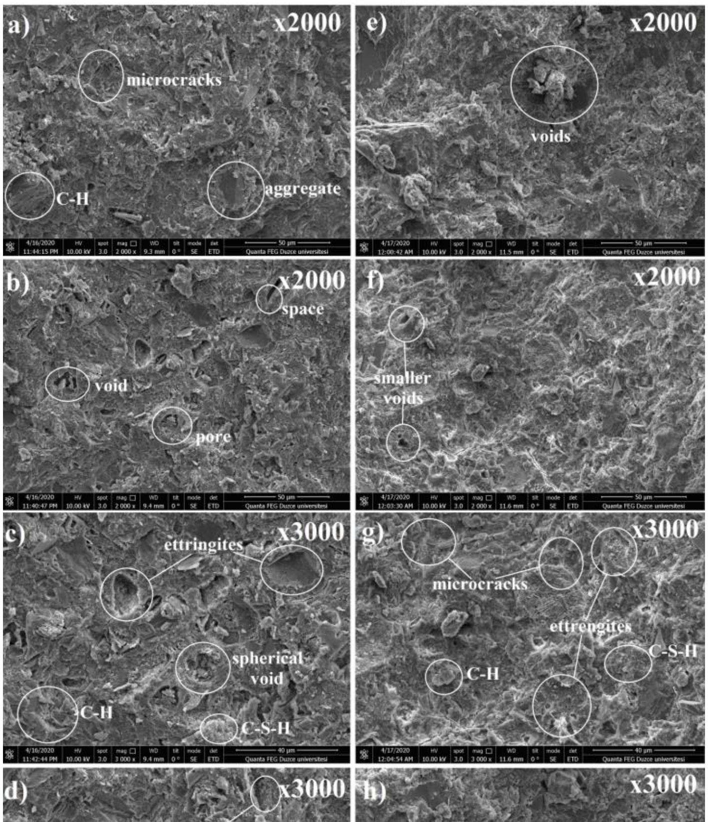

Fig. 4. SEM images of the fractured surfaces obtained from the compressive strengths tests of C25/30 (a, b, c and d) and C30/37 (e, f, g and h). concrete samples

4. Conclusion

In the present work, the crucial characteristic properties of the concretes samples (C25/30, C30/37 and C35/45) produced with the usage of the aggregates obtained from Çatakören region were studied in detail. The all features of all the components composed of the concretes were investigated by means of the relevant standards. Namely, chemical and physical properties of the cement, characteristic properties of the set accelerating admixture, water reducing admixture character were determined. Furthermore, the physical, qualitative mineralogical, petro-graphic, X-ray diffraction, mechanical besides the grain size distribution limits properties of the aggregates were characterized in detail. In addition to that, the compressive strength, slump grade, apparent density results of the all types of the concretes revealed that the aggregates produced from Çatakören region was considerable proper and usable for the production of the concretes meeting the standards. Furthermore, SEM analysis depicted that there existed better interfacial adhesion and stronger chemical bonds were formed in the concrete matrix in C30/37 concrete with the decrements in the porosity. Furthermore, the formation of voids, spaces, ettringites as well as microcracks were observed in the images belonging to each classes of the concretes.

Acknowledgement

This work was supported by Bolu Abant Izzet Baysal University. The author thanks to Bolu Ready-Mixed Concrete Facility for their valuable helps, supports besides the experimental measurements.

References

Campelo, N. D., Campos, A. M. L. D., Aragao, A. F., 2019. Comparative Analysis of Asphalt Concrete Mixtures Employing Pebbles and Synthetic Coarse Aggregate of Calcined Clay in the Amazon Region. International Journal of Pavement Engineering, 20(5): 507-518.

de Oliveira, A. A., Pimentel, M. G., Picanco, M. D., 2019. Mechanical Properties and Microstructural Analysis of a Concrete Produced with Aggregate from the Brazilian Amazon Region. Matéria (Rio de Janeiro), 24(4): e12513.

Eui-Hwan, H., Ko, Y. S., Jeon, J. K., 2007. Effect of Polymer Cement Modifiers on Mechanical and Physical Properties of Polymer-Modified Mortar using Recycled Waste Concrete Fine Aggregate. Journal of Industrial and Engineering Chemistry, 13(3): 387-394.

Evangelista, L., Guedes, M., de Brito, J., Ferro, A. C., Pereira, M. F., 2015. Physical, Chemical and Mineralogical Properties of Fine Recycled Aggregates Made from Concrete Waste. Construction and Building Materials, 86: 178-188.

Gencel, O., 2011. Physical and Mechanical Properties of Concrete Containing Hematite as Aggregates. Science and Engineering of Composite Materials, 18(3): 191-199.

Halvaei, M., Jamshidi, M., Latifi, M., 2016. Effect of Fiber Geometry and Tenacity on the Mechanical Properties of Fine Aggregates Concrete. Journal of Industrial Textiles, 45(5): 1083-1099.

Kakae, N., Miyamoto, K., Momma, T., Sawada, S., Kumagai, H., Ohga, Y., Abiru, T., 2017. Physical and Thermal Properties of Concrete Subjected to High Temperature. Journal of Advanced Concrete Technology, 15(6): 190-212.

Leman, A. S., Shahidan, S., Yusuf, M. Y., Zuki, S. S. M., Misnon, N. A., 2017. Workability and Compressive Strength for Concrete with Coconut Shell Aggregate. 9th International Unimas Stem Engineering Conference (Encon 2016) Innovative Solutions for Engineering and Technology Challenges, 87.

Liu, H. L., Shi, J. J., Qu, H. Q., Ding, D. X., 2019. An Investigation on Physical, Mechanical, Leaching and Radiation Shielding Behaviors of Barite Concrete Containing Recycled Cathode Ray Tube Funnel Glass Aggregate. Construction and Building Materials, 201: 818-827.

Liu, X. A., Guan, J. A., Wang, Z. M., Ren, X. W., Cui, S. P., 2016. Compatibility of Polycarboxylate Superplasticizer with Raw Materials of Concrete. 1st International Conference on Uhpc Materials and Structures, 105: 83-94.

Lyu, B. C., Wang, A. G., Zhang, Z. H., Liu, K. W., Xu, H. Y., Shi, L., Sun, D. S., 2019. Coral Aggregate Concrete: Numerical Description of Physical, Chemical and Morphological Properties of Coral Aggregate. Cement & Concrete Composites, 100: 25-34.

Marthong, C., Sangma, A. S., Choudhury, S. A., Pyrbot, R. N., Tron, S. L., Mawroh, L., Bharti, G. S., 2017. Structural Behavior of Recycled Aggregate Concrete Beam-Column Connection in Presence of Micro Concrete at Joint Region. Structures, 11: 243-251.

Ramdani, S., Guettala, A., Benmalek, M. L., Aguiar, J. B., 2019. Physical and Mechanical Performance of Concrete Made with Waste Rubber Aggregate, Glass Powder and Silica Sand Powder. Journal of Building Engineering, 21: 302-311.

Roy, S., Miura, T., Nakamura, H., Yamamoto, Y., 2020. High Temperature Influence on Concrete Produced by Spherical Shaped Eaf Slag Fine Aggregate - Physical and Mechanical Properties. Construction and Building Materials, 231: 117153.

Sahin, R., Akarsu, M., 2011. Compatibility of Coarse Aggregates with Different Cements for Key Characteristics of Self-Compacting Concrete. Indian Journal of Engineering and Materials Sciences, 18(3): 239-247.

Sokhansefat, G., Ley, M. T., Cook, M. D., Alturki, R., Moradian, M., 2019. Investigation of Concrete Workability through Characterization of Aggregate Gradation in Hardened Concrete using X-Ray Computed Tomography. Cement & Concrete Composites, 98: 150-161.

Soykan, U., Cetin, S., 2015. Reinforcement of High Density Polyethylene with a Side Chain LCP by Graft Copolymerization-Thermal, Mechanical and Morphological Properties. Journal of Polymer Research, 22: 204.

Stroeven, P., Hu, J., 2006. Review Paper - Stereology: Historical Perspective and Applicability to Concrete Technology. Materials and Structures, 39(1): 127-135.

Ueno, A., Ogawa, Y., 2020. Influence of Coarse Aggregate Shape on Optimum Fine to Total Aggregate Ratio using A Virtual Voids-Ratio Diagram in Concrete Compaction. Cement & Concrete Composites, 106: 103463.